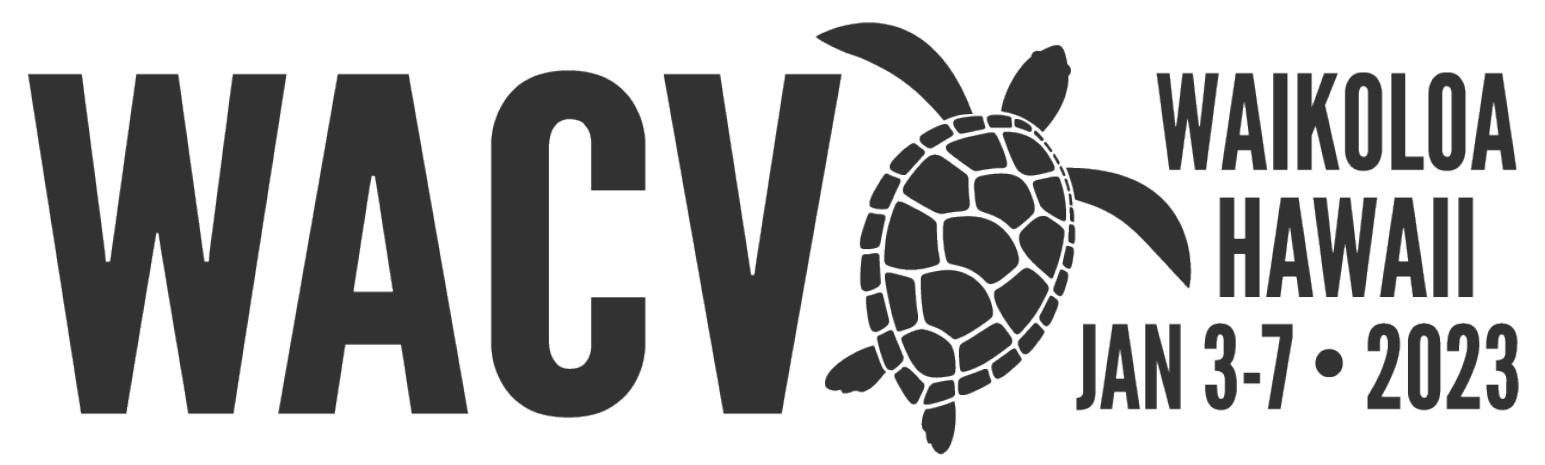


Learning 3D Human Pose Estimation from Dozens of Datasets using a Geometry-Aware Autoencoder to Bridge Between Skeleton Formats



István Sáránci, Alexander Hermans, Bastian Leibe



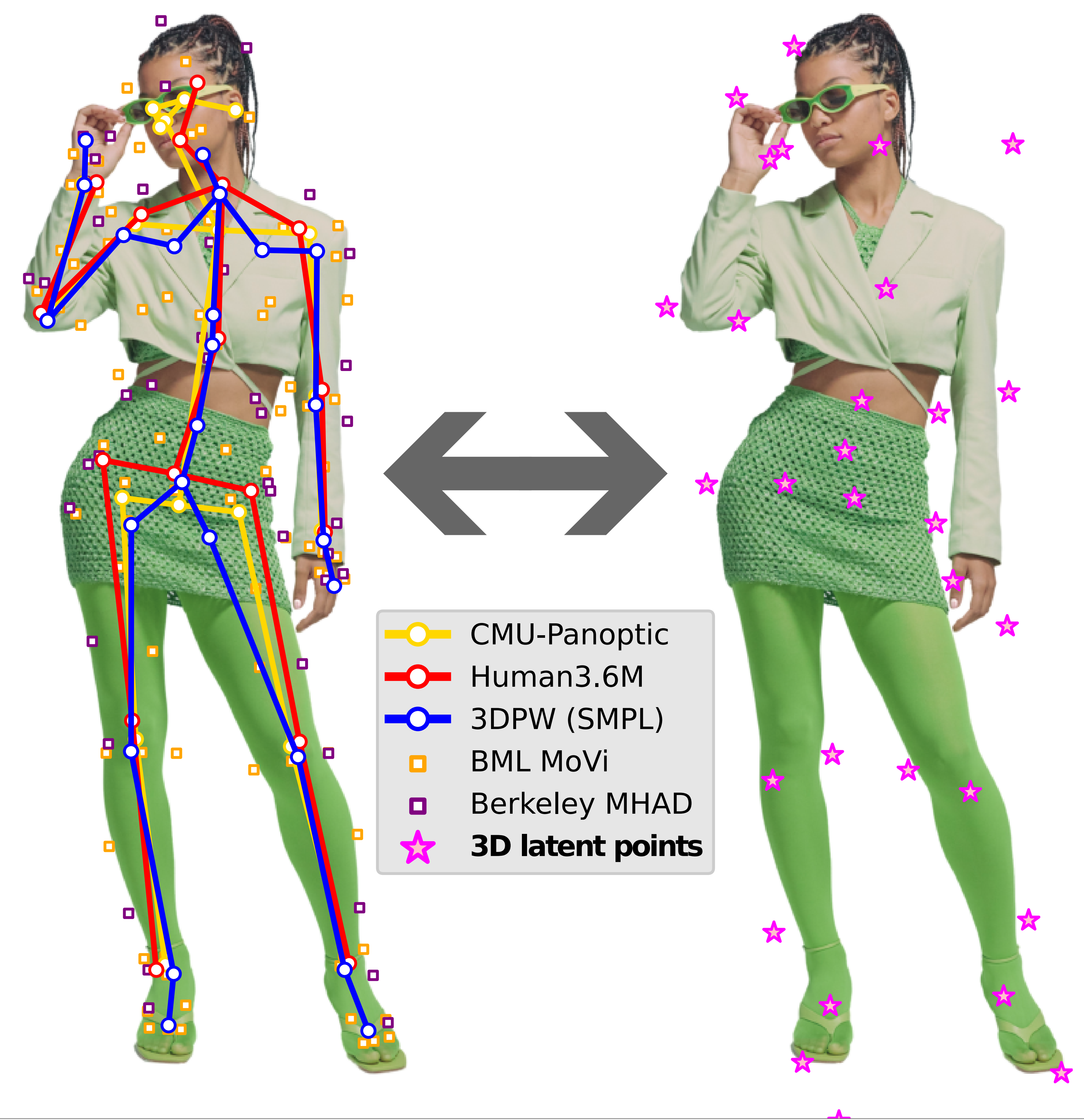
TL;DR We discover how various 3D human **skeleton formats** are related, via a novel **affine-combining autoencoder**, enabling **extreme multi-dataset 3D pose training**. We release **strong 3D pose estimators** for downstream research.



vision.rwth-aachen.de/wacv23sarandi

The Problem

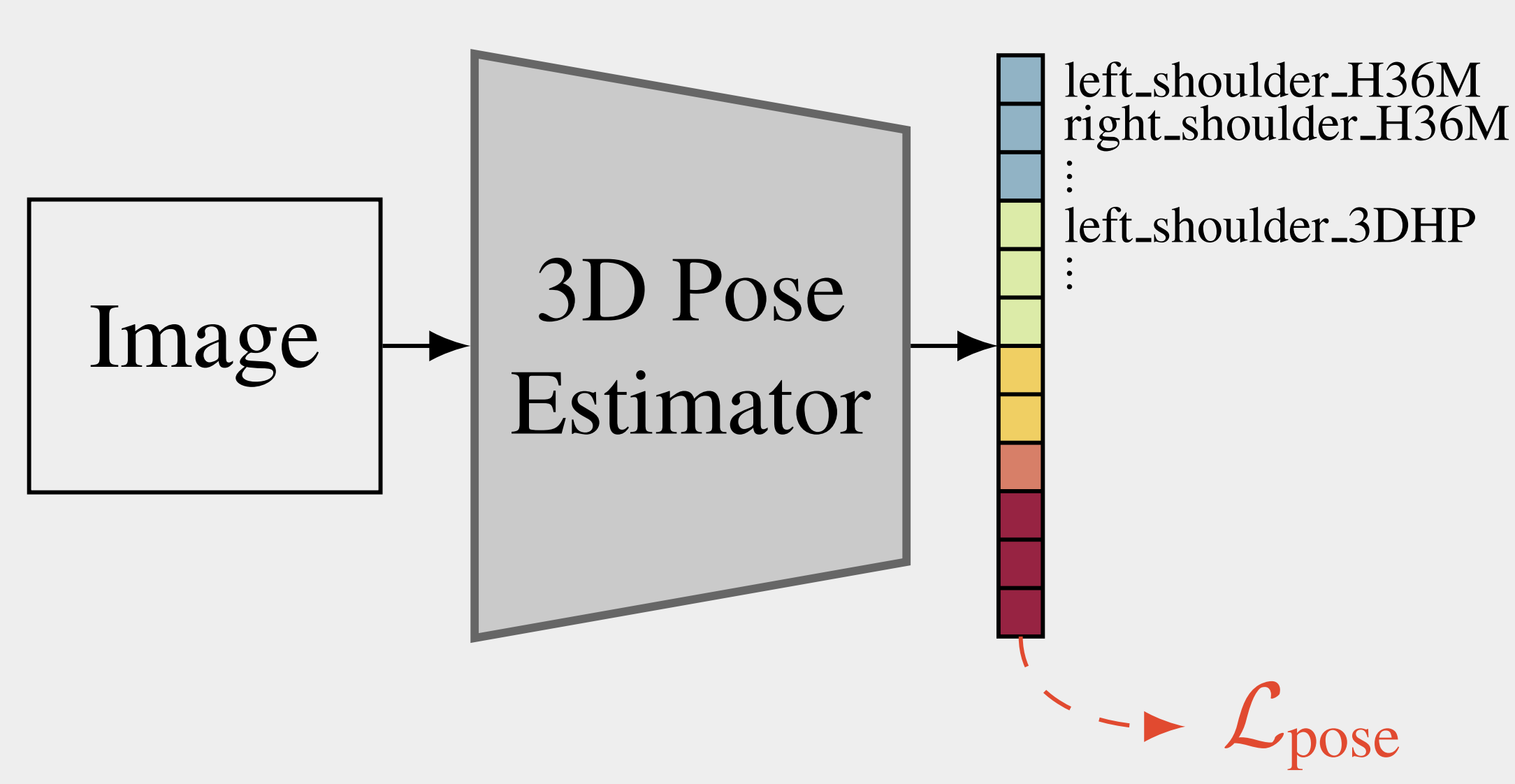
- Single RGB image → 3D human pose
- **Lack of data** is seen as a big problem
- This led many to focus on 2D-to-3D lifting and self-supervision
- Instead, we **push the fully-supervised regime** to the extreme
- Actually, **lots of datasets** exist now – let's use **28!** (see bottom)
- But datasets use **different skeleton formats!** →
- Unclear how to **supervise one model** with them
- Idea: learn **how the skeleton definitions relate**
- Goal: effective information sharing across formats



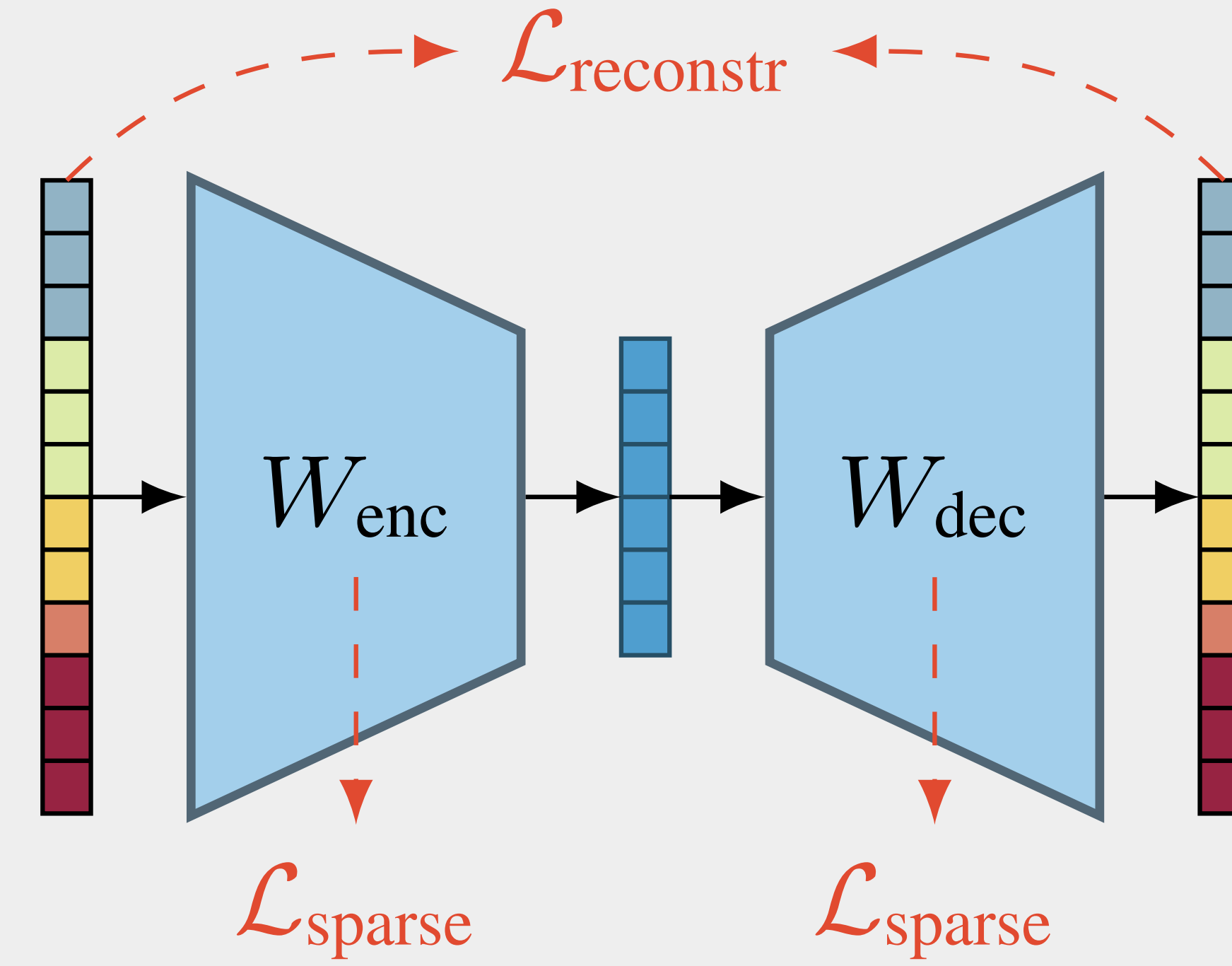
Approach

- Discover **latent 3D points** that best explain all formats
- Design a novel but simple **geometric autoencoder** for this
- Use pseudo-GT with **multiple formats per sample** to train autoencoder

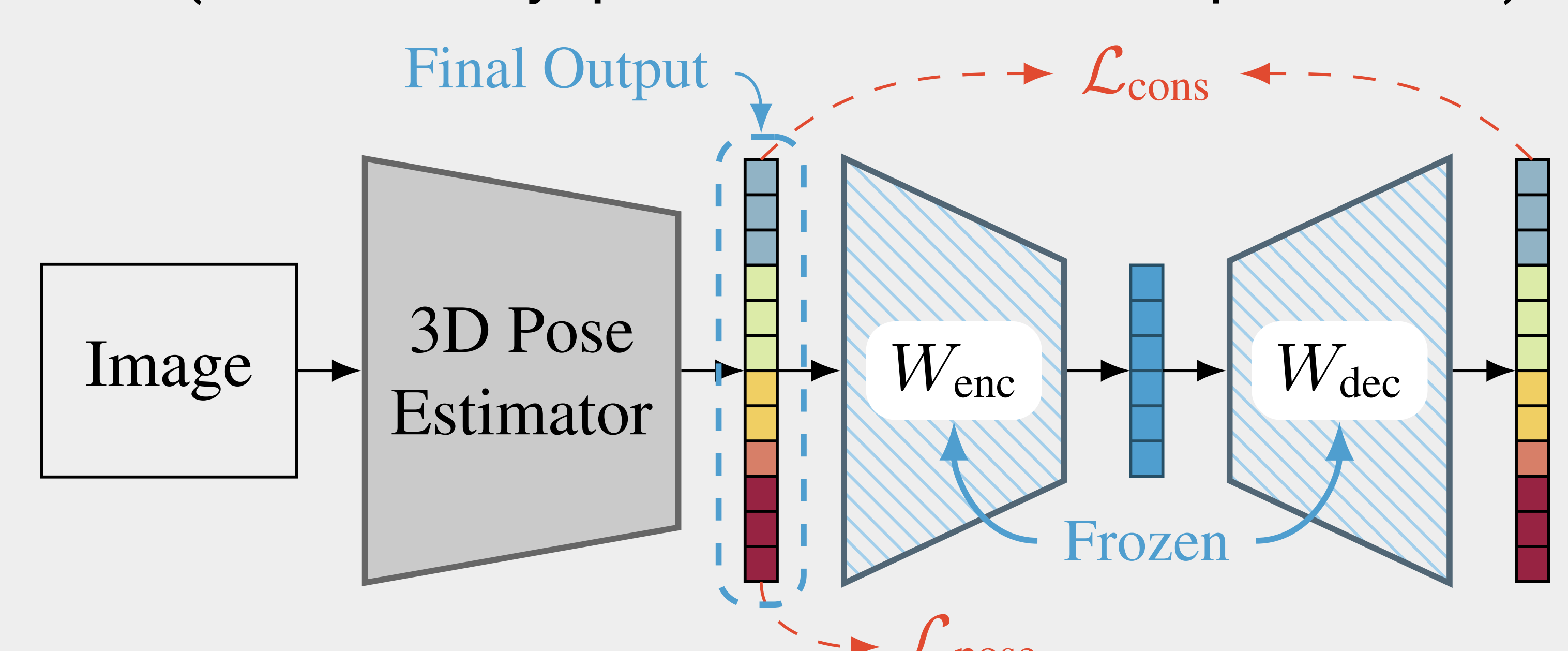
Step 1) Train a multi-dataset model with separate output heads per skeleton format, to **pseudo-annotate images with all formats**



Step 2) Train our **affine-combining autoencoder** to discover relations between formats by compressing them to a **latent keypoint set**



Step 3) Consistency-regularization: make the model predict poses near the latent space (alternatively: perform direct latent prediction)



Affine-Combining Autoencoder (ACAE)

- **Want: equivariance** to rotation, translation, scale, chirality
- **Linear, constrained, regularized autoencoder**
- Constraint 1) same weights for X, Y, Z coordinates
- Constraint 2) weights sum to one (affine combination)
- Regularization loss: L1 for sparsity
- Reconstruction loss: L1
- **Generally applicable** to compress large sets of keypoints

$$\text{minimize}_{W_{\text{enc}} \in \mathbb{R}^{L \times J}, W_{\text{dec}} \in \mathbb{R}^{J \times L}} \mathcal{L}_{\text{reconstr}} + \lambda_{\text{sparse}} \mathcal{L}_{\text{sparse}}$$

$$\mathcal{L}_{\text{reconstr}} = \frac{1}{K} \sum_{k=1}^K \|P_k - W_{\text{dec}} W_{\text{enc}} P_k\|_1$$

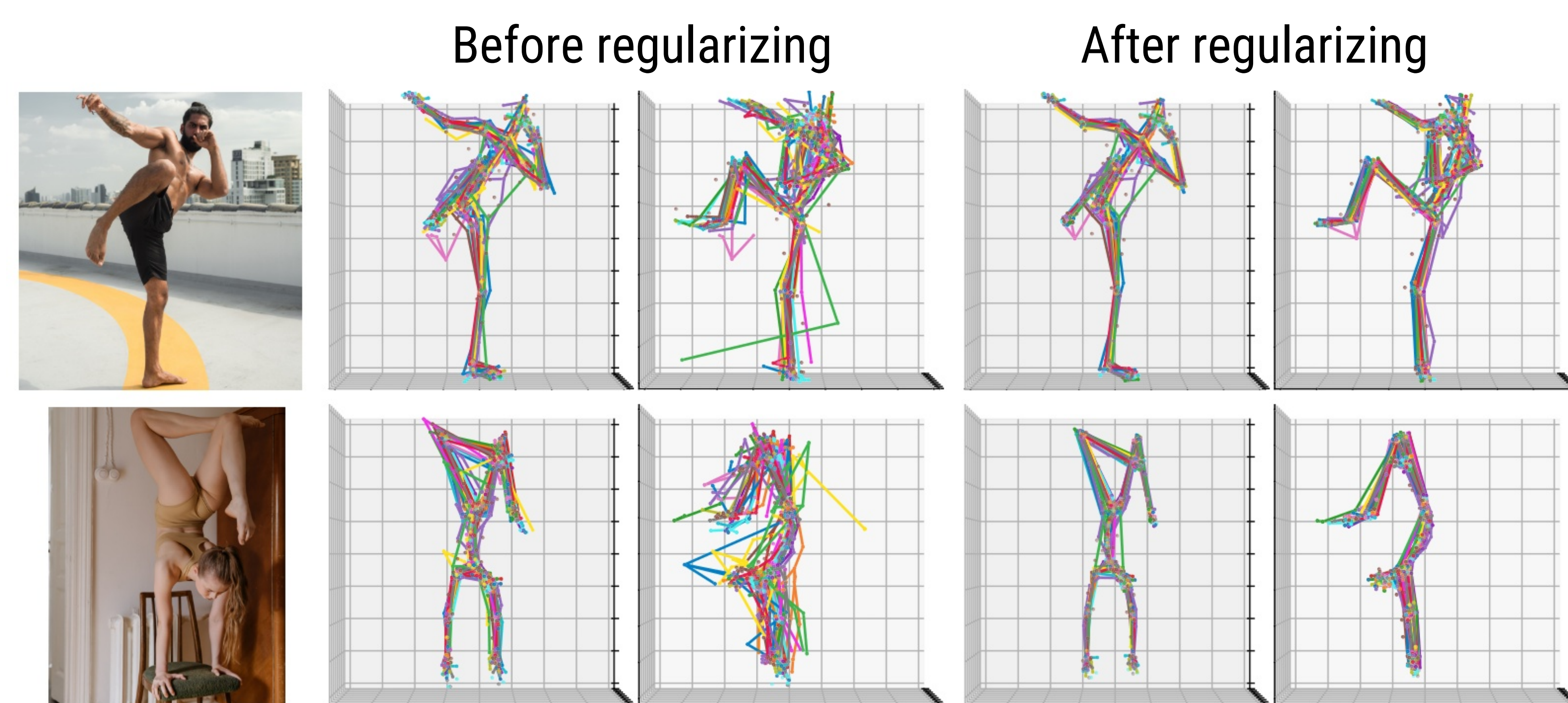
$$\mathcal{L}_{\text{sparse}} = \|W_{\text{enc}}\|_1 + \|W_{\text{dec}}\|_1$$

$$\text{s. t. } W_{\text{enc}} \mathbf{1}_J = \mathbf{1}_L, \quad W_{\text{dec}} \mathbf{1}_L = \mathbf{1}_J,$$

Findings

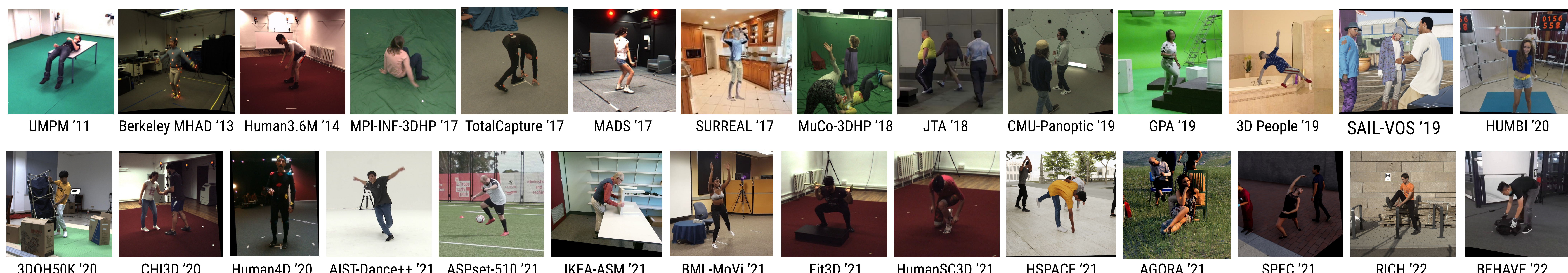
- Base model is our **MeTRAbs** pose estimator
- **Data scale helps!** Steady improvement with 1 → 3 → 14 → 28 ds.
- Separate skeleton output heads give inconsistent depth predictions
- **ACAE consistency-regularization improves consistency**
- **Models become much stronger** than those from prior work
- Models available at vision.rwth-aachen.de/wacv23sarandi

| | MuPoTS-3D | | | | 3DPW | | | | MPI-INF-3DHP | | | | Human3.6M | | | |
|----------------------------|-------------|-------------|----------------------|----------------------|-------------|-------------|----------------------|----------------------|--------------|-------------|----------------------|----------------------|-------------|-------------|----------------------|----------------------|
| | MJPEL | PMPJPEL | PCK ₁₀₀ ↑ | CPS ₂₀₀ ↑ | MJPEL | PMPJPEL | PCK ₁₀₀ ↑ | CPS ₂₀₀ ↑ | MJPEL | PMPJPEL | PCK ₁₀₀ ↑ | CPS ₂₀₀ ↑ | MJPEL | PMPJPEL | PCK ₁₀₀ ↑ | CPS ₂₀₀ ↑ |
| Merged joints | 91.9 | 67.3 | 63.2 | 69.9 | 72.5 | 48.3 | 79.5 | 69.7 | 69.8 | 51.6 | 80.7 | 79.4 | 44.6 | 34.2 | 93.9 | 89.8 |
| Separate joints (F. 3a) | 84.6 | 59.0 | 70.1 | 66.0 | 61.8 | 43.4 | 83.8 | 71.1 | 59.6 | 44.1 | 86.6 | 81.8 | 44.7 | 34.3 | 94.3 | 90.1 |
| Consistency regul. (F. 3c) | 81.8 | 57.8 | 72.5 | 72.9 | 61.5 | 43.0 | 84.0 | 71.9 | 59.2 | 43.6 | 86.6 | 82.7 | 45.2 | 33.3 | 94.4 | 90.1 |
| Latent pred. (F. 4a) | 83.0 | 58.9 | 71.4 | 71.2 | 62.0 | 43.6 | 84.0 | 71.7 | 60.2 | 44.7 | 86.1 | 80.2 | 46.5 | 34.4 | 93.9 | 89.5 |
| Hybrid (F. 4b) | 82.7 | 58.5 | 71.6 | 72.1 | 61.8 | 43.3 | 84.0 | 71.8 | 60.4 | 44.8 | 85.9 | 80.9 | 46.1 | 34.2 | 94.1 | 89.4 |
| Separate joints | 82.9 | 57.7 | 71.0 | 70.9 | 60.9 | 42.1 | 84.4 | 73.4 | 59.1 | 42.2 | 88.0 | 85.3 | 41.6 | 32.0 | 95.1 | 92.1 |
| Consistency regul. | 81.0 | 57.4 | 72.8 | 74.8 | 60.6 | 41.7 | 84.7 | 74.3 | 57.9 | 41.8 | 88.2 | 84.7 | 40.6 | 30.7 | 95.7 | 92.6 |
| Hybrid | 81.3 | 57.9 | 72.4 | 73.9 | 61.1 | 42.0 | 84.6 | 74.3 | 59.2 | 42.8 | 87.2 | 84.3 | 41.8 | 31.4 | 95.6 | 92.6 |



| | MuPoTS-3D | | 3DPW | | MPI-INF-3DHP | | Human3.6M |
|---|----------------------|--------|---------|---------------------|--------------|----------------------|-----------|
| | PCK ₁₅₀ ↑ | MPJPE↓ | PMPJPE↓ | PCK ₅₀ ↑ | MPJPE↓ | PCK ₁₅₀ ↑ | MPJPE↓ |
| Sun <i>et al.</i> (2021) | – | 80.1 | 56.8 | 36.5 | – | – | – |
| Lin <i>et al.</i> (2021b) | – | 74.7 | 45.6 | – | – | – | 51.2 |
| Gong <i>et al.</i> (2021) | – | – | – | – | 71.1 | 89.2 | 50.2 |
| Cheng <i>et al.</i> (2022) | 89.6 | – | – | – | – | – | 49.3 |
| <i>Ours with crop resolution 256x256 and 400k steps</i> | | | | | | | |
| ResNet-50 | 92.2 | 65.5 | 47.2 | 49.0 | 64.2 | 93.3 | 45.8 |
| EffNetV2-S | 93.7 | 61.5 | 43.0 | 51.8 | 60.0 | 95.3 | 45.2 |
| EffNetV2-L | 94.1 | 60.6 | 41.7 | 52.1 | 59.2 | 95.8 | 40.6 |
| <i>Ours with crop resolution 384x384 and 800k steps</i> | | | | | | | |
| EffNetV2-S | 94.9 | 59.5 | 41.0 | 53.1 | 58.7 | 96.2 | 41.4 |
| EffNetV2-S 5-crop TTA | 95.2 | 58.9 | 39.9 | 53.6 | 57.5 | 96.7 | 40.1 |
| EffNetV2-L | 95.4 | 58.9 | 39.5 | 53.9 | 55.4 | 97.1 | 36.5 |
| EffNetV2-L 5-crop TTA | 95.7 | 57.0 | 38.1 | 55.4 | 53.6 | 97.6 | 35.5 |

The Used Datasets



Acknowledgments. This work was supported by the ERC Consolidator Grant project "DeeViSe" (ERC-CoG-2017-773161) and by Robert Bosch GmbH under the project "Context Understanding for Autonomous Systems".